Complete characterization of a Si(Li) detector in the photon energy range 0.9–5 keV

M. Krumrey,

BESSY mbH, Lentzeallee 100, D-1000 Berlin 33, Germany

E. Tegeler and G. Ulm

Physikalisch-Technische Bundesanstalt, Abbestrasse 2-12, D-1000 Berlin 10, Germany

(Presented on 31 August 1988)

The response function of a Si(Li) detector has been measured in the photon energy range 0.9–5 keV using monochromatized synchrotron radiation at a double crystal monochromator. The response is described by a HYPERMET function and the spectral dependence of its parameters is presented. The quantum detection efficiency of the detector is determined from measurements in the undispersed synchrotron radiation of the electron storage ring BESSY, which is a primary radiometric standard.

INTRODUCTION

Energy dispersive photon counting systems are used in the x-ray and γ-ray region for various applications in material research, radiometry, nuclear physics, and environmental studies. Also, in the spectral region below 5 keV, there are several extremely useful applications of Si(Li) detectors, particularly for applications at synchrotron radiation (SR) facilities:

(i) Though the energy resolution of energy dispersive Si(Li) detectors is only of the order of $\Delta E = 100$ eV, this is sufficient for the separation of higher order contributions of monochromators for photon energies $h\nu > 200$ eV. Therefore, Si(Li) detectors can be used for the characterization of grazing incidence grating monochromators and crystal monochromators.

(ii) Si(Li) detectors can be used for the detection and identification of characteristic x rays for all elements with $Z > 4$, i.e., also for the very important elements; carbon, nitrogen, and oxygen. Therefore, SR induced x-ray fluorescence identified with a suitable Si(Li) detector is a powerful tool in material research. Also, for the application of EXAFS techniques to surface physics, the measurement of fluorescence emission of surface atoms instead of transmittance measurements offers several advantages.

We see two central reasons why Si(Li) detectors are up to now not widely used at SR centers in the region below 5 keV:

(i) Due to the demands of their main customers, the manufacturers of Si(Li) detectors have optimized their systems for nuclear physics and material research. Although there are no principal technical difficulties, ultrahigh vacuum compatible systems are not offered, and due to bad vacuum conditions an increasing layer of ice on the permanently cooled detector is observed.[1,2] This problem can be solved by the manufacturers if there is a growing market for adequate detector systems.

(ii) The unique potential of Si(Li) detectors can only be utilized if the detector is completely characterized, i.e., if the response function $p(h\nu,E)$ and the quantum detection efficiency $\epsilon(h\nu)$ are known. Here, $h\nu$ is the energy of the incident photons and E refers to the energy axes of the multichannel analyzer (MCA) used for data acquisition. The conventional methods for the characterization of Si(Li) detectors are mainly based on calibrated radioactive sources[3] which are not available in the soft x-ray region.

The measurement of $p(h\nu,E)$ has to be performed with monochromatic radiation of different photon energies $h\nu$, while, for the determination of $\epsilon(h\nu)$, radiation of known spectral photon flux is required. At the electron storage ring BESSY, both requirements can be fulfilled: Monochromatic radiation is available at various monochromators, and a precisely known photon flux is emitted from the storage ring which is a primary radiation standard.[4] Although for the complete characterization of a Si(Li) detector we used a detector with a 7.6-μm Be window, the spectral range can easily be extended to lower photon energies if a detector without or with an ultrathin window is used.

I. RESPONSE FUNCTION

For the determination of the response function, the Si(Li) detector was irradiated with monochromatic radiation between 0.9 and 5 keV at the BESSY double crystal monochromator.[5] At normal operation conditions of BESSY (electron energy 756 MeV, electron current 300 mA), the monochromatic photon flux behind the monochromator is of the order of some 10^{10} photons/s, while the count rate of the Si(Li) detector is limited to a few thousand counts per second. Therefore, the measurements for the determination of the response function were performed with BESSY operated at an electron current of a few microamps or less.

The response of the Si(Li) detector to monochromatized radiation of photon energy $h\nu$ as registered with the MCA can be seen for four different photon energies from Fig. 1. As discussed in the Introduction, this measurement is not only a characterization of the energy dispersive detector, but also of the monochromator: For the measurements at photon energies below 1.8 keV, where beryl crystals have been used as dispersive elements, the higher order contributions are not negligible. At photon energies above 1.8 keV

 0034-6748/89/072287-04$01.30

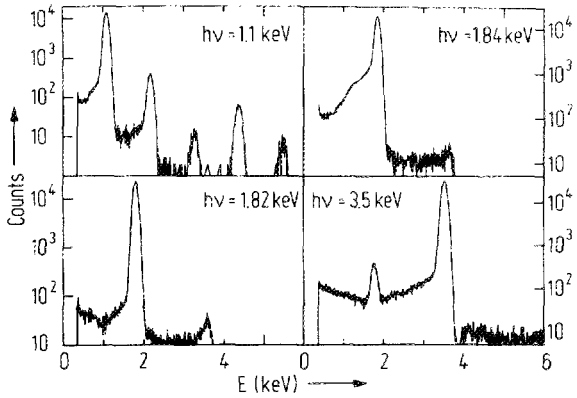

FIG. 1. Measured response of the Si(Li) detector system to "monochromatized" radiation behind a double crystal monochromator at the storage ring BESSY. For the measurement at 1100 eV a Beryl crystal was used, for the other measurements an InSb crystal was used. The count rate was of the order to 1000 cps.

where an InSb crystal was utilized, no significant higher order contributions are present. A drastic change is observed in the response function at the Si K absorption edge: Above the absorption edge a very pronounced low-energy tail is observed, as can be seen from the spectrum obtained at $h\nu = 1840$ eV. Additionally, for higher photon energies, the well-known escape peak shows up.

The shape of the response $p(h\nu,E)$ is a Gaussian peak centered at $E = h\nu$ with a low-energy tail. As it has been discussed by several authors,[6,7] $p(h\nu,E)$ can be approximated by a modified HYPERMET function $F(E)$ with

$$F(E) = G(E) + S(E) + D(E) + \mathrm{Esc}(E) + T(E), \tag{1}$$

with the full energy Gaussian peak $G(E)$

$$G(E) = H_G \exp[-(E - h\nu)^2/2\sigma^2], \tag{1a}$$

the step function $S(E)$

$$S(E) = H_S \tfrac{1}{2}\{1 - \mathrm{erf}[(E - h\nu)/\sigma\sqrt{2}]\}, \tag{1b}$$

the exponential tail function $D(E)$

$$D(E) = H_D \tfrac{1}{2} \exp[(E - h\nu)/\beta] \times \{1 - \mathrm{erf}[(E - h\nu)/\sigma\sqrt{2} + \sigma/\beta\sqrt{2}]\}, \tag{1c}$$

the escape peak centered at the energy E_{Esc}

$$\mathrm{Esc}(E) = H_{\mathrm{Esc}} \exp[-(E_{\mathrm{Esc}} - E)^2/2\sigma^2], \tag{1d}$$

and the signal correlated noise function $T(E)$

$$T(E) = H_T E^{-1.2}. \tag{1e}$$

The exponent -1.2 of the noise function has been determined in advance by a fitting code, which is based on the algorithm CURFIT.[8] We have included the noise function in the response function, because we found that the noise is correlated with photons of the energy under consideration and has nothing to do with high-energy radiation as stated by other authors.[7] The counts registered at photon energies above the full energy peak depend on the count rate and will not be considered in the following discussion.

The approximation of the measured response function at $h\nu = 3500$ eV by this modified HYPERMET function and the individual components of the HYPERMET function can be seen from Fig. 2. For the characterization of the detector, the spectral dependence of the parameters in the HYPERMET function has to be determined. For all measured responses of the detector to the "monochromatic" radiation behind the crystal monochromator, we determined the parameters of the HYPERMET function with a standard fit procedure.[8] In Fig. 3, the spectral dependences of the most important parameters are shown together with the approximation by simple mathematical expressions (solid lines), which have a justification from the physics of the semiconductor Si(Li) detector, at least in some cases.[9]

Since we do not know the absolute photon flux behind the crystal monochromator, we cannot determine H_G which is correlated to the quantum detection efficiency. For their presentation in Fig. 3, all intensity factors H are normalized to H_G.

The width of the response function is given by parameters σ (or $\Delta_{\mathrm{FWHM}} = 2.355\,\sigma$) for the full energy Gaussian peak $G(E)$ and the parameter β in the tail function $D(E)$. We fitted the spectral dependence of the halfwidth with the usual approach.[10]

$$\Delta^2_{\mathrm{FWHM}} = \Delta^2_{el} + (2.355)^2 F\epsilon h\nu, \tag{2}$$

with ϵ being the average energy for the creation of an electron hole pair (3.81 eV for Si at 77 K). For our detector system, we found $\Delta_{el} = 121$ eV for the electronic part and $F = 0.072$ for the Fano factor.

While σ is continuously increasing with the photon energy, we found a change in the ratio β/σ at the Si K absorption edge. Since the existence of an exponential tail is caused by the absorption in Si, H_D/H_G shows an enormous jump at the Si K absorption edge. The intensity H_T/H_G of the signal correlated noise $T(E)$ also shows a weak structure at the Si K absorption edge.

The step function $S(E)$ seems to be correlated with the absorption of the Au contact at the surface of the detector crystal, because we found significant contributions only for photon energies $h\nu > 2206$ eV, the onset of the Au M absorption. The escape peak could only be identified for photon energies $h\nu > 2300$ eV, and the ratio H_{Ecs}/H_G is in good agreement with the model suggested by Johannsen.[11] In

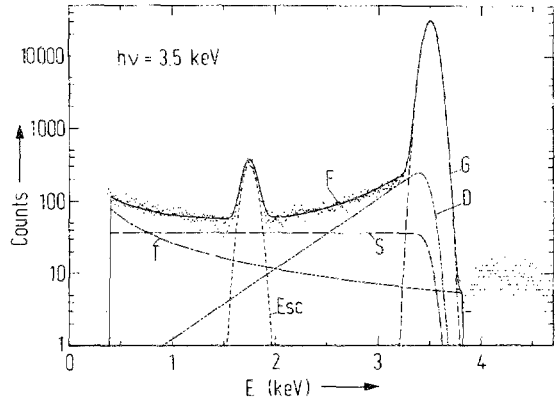

FIG. 2. Approximation of the measured response of the detector system at 3.5 keV (dots) with the modified HYPERMET function $F(E)$ and the individual components of the HYPERMET function: full energy Gaussian peak $G(E)$, step function $S(E)$, exponential tail $D(E)$, escape peak $\mathrm{Esc}(E)$, and signal correlated noise $T(E)$.

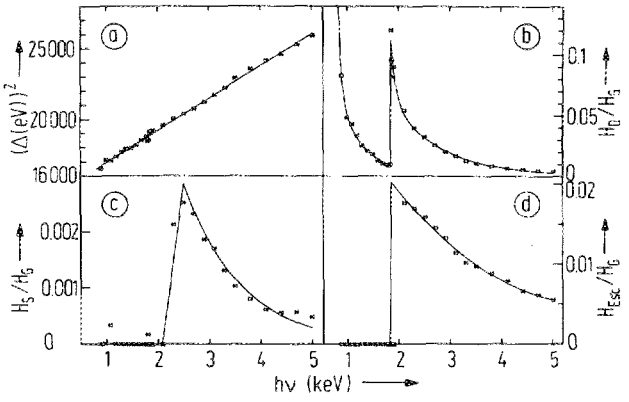

FIG. 3. Spectral dependence of the most important parameters in the components of the HYPERMET function. (a) Δ_{FWHM} of the full energy Gaussian peak, (b) H_D/H_G (exponential tail function), (c) H_S/H_G (step function), and (d) H_{Esc}/H_G (escape function).

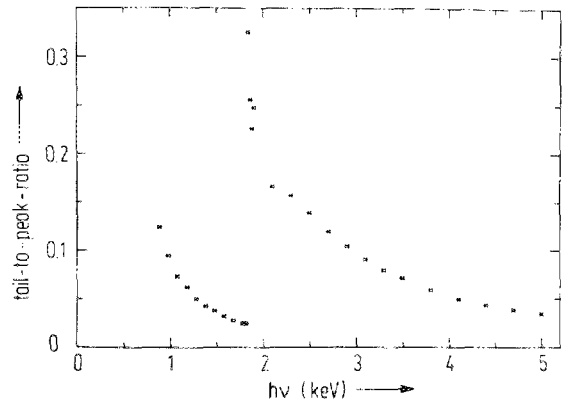

FIG. 4. Number of counts in the "tail" relative to the number of counts in the full energy Gaussian peak.

agreement with other authors,[12] we found the energy shift $\Delta_{Esc} = h\nu - E_{Esc} = 1749$ eV instead of 1740 eV as expected from the energy of the Si K emission.

If we separate all counts registered with the MCA for energies $E > 600$ eV into counts within the Gaussian peak $G(E)$ ("peak") and counts outside of $G(E)$ ("tail"), we find a correlation of the tail-to-peak ratio with the absorption of Si (see Fig. 4). The tail-to-peak ratio reaches values up to 0.3 just above the Si K absorption edge. Extreme care, therefore, has to be taken using a Si(Li) detector for absolute photon flux measurements in this spectral region.

II. THE QUANTUM DETECTION EFFICIENCY $\epsilon(h\nu)$

For quantitative measurements, the quantum detection efficiency $\epsilon(h\nu)$ has to be known. In accordance with the literature,[13] we define $\epsilon(h\nu)$ to be the probability that a photon of energy $h\nu$ passing the aperture in front of the detector leads to a pulse which can be attributed to the full energy Gaussian peak $G(E)$.

The quantum detection efficiency $\epsilon(h\nu)$ can be determined by measuring the response of the detector system to a known spectral photon flux $N_{h\nu}(h\nu)$. As standard radiation sources like radioactive sources cannot be used for photon energies below 5 keV, we used the undispersed SR of the electron storage ring BESSY, which is a radiometric standard with small uncertainties in the soft x-ray range.[4,14] Since the count rate of the Si(Li) detector may not exceed 1000 cps to avoid pileup pulses, the storage ring has to be operated with only a few electrons stored, which must be counted precisely for the calculation of the spectral photon flux. During our measurements, the energy of the stored electrons was $W = (755.65 \pm 0.4)$ MeV, the limiting circular aperture of the detector had a radius $r = (1.239 \pm 0.005)$ mm and was situated in the center of the vertical angular distribution of the SR at a distance $d = (6078 \pm 10)$ mm from the source point of the SR. The resulting uncertainty of $\epsilon(h\nu)$ in the soft x-ray range between 1–5 keV is of the order 3%, details are discussed elsewhere.[4,14]

In an energy dispersive photon counting system, a spectral photon flux $N_{h\nu}(h\nu)$ leads to a spectral count rate $C_E(E)$. $C_E(E)$ and $N_{h\nu}(h\nu)$ are related by

$$C_E(E) = \int N_{h\nu}(h\nu) \cdot \epsilon(h\nu) \cdot p(h\nu,E) dh\nu, \tag{3}$$

where $p(h\nu,E)$ is approximated by the HYPERMET function $F(E)$.

From the definition of $\epsilon(h\nu)$ we have

$$\int p(h\nu,E) dE = 1 + \text{tail-to-peak ratio} > 1. \tag{4}$$

Therefore, Eq. (3) is a convolution which does not preserve the integral count rate.

If the spectral count rate $C_E(E)$ induced by a known photon flux $N_{h\nu}(h\nu)$ is measured, $\epsilon(h\nu)$ can be determined from Eq. (3). Because the SR is a broadband continuum and the halfwidth of the response function $p(h\nu,E)$ is much larger than the spectral width of the structures in $\epsilon(h\nu)$, which can be measured in monochromatic radiation behind a monochromator, a deconvolution procedure according to Eq. (3) does not lead to satisfactory results in the vicinity of structures in $\epsilon(h\nu)$, especially in the vicinity of the Si K absorption edge. On the other hand, reliable models for the calculation of $\epsilon(h\nu)$ are described in the literature.[13] We therefore determine $\epsilon(h\nu)$ according to the following procedure: $\epsilon(h\nu)$ is calculated from a model function with several free parameters. Using an iterative fit procedure, the free parameters are chosen in such a way that with a convolution according to Eq. (3) the experimental data are described as accurately as possible.

The physical model for the calculation of $\epsilon(h\nu)$ is rather simple: Every photon which is absorbed in the depletion layer of the detector will produce a pulse in the full energy Gaussian peak, except for escape effects. Therefore, one only has to take into account absorption in filters, windows, and dead layers in front of the depletion layer of the detector crystal. The quantum detection efficiency $\epsilon(h\nu)$ therefore is given by

$$\epsilon(h\nu) = \tau_{Be}(h\nu)\tau_0(h\nu)\tau_{Au}(h\nu)\tau_{Si}(h\nu)f_{Esc}(h\nu) \times [1 - \tau_{pn}(h\nu)], \tag{5}$$

where τ denotes the transmittance of a 7.6-μm Be window, a 1.6-μm layer of water ice which is dominated by the absorption of oxygen, an Au contact of thickness 21 nm, and a Si deadlayer of 370 nm. The escape pulses are taken into ac-

count by $f_{Esc}(h\nu)$. In the spectral region investigated in this paper, the transmittance τ_{pn} of the depletion layer can be neglected. The absorption data for the absorbing layers have been taken from the literature,[15,16] the thickness of these layers are the only free parameters. The thicknesses of the various layers as given above are in the best agreement with our measurements and, also, in good agreement with the manufacturer's specifications and values that can be derived from the parameters of the response function presented in the previous chapter.

The quantum detection efficiency calculated according to Eq. (5) is shown in the upper part of Fig. 5, whereas the lower part demonstrates the agreement between the spectral count rates $C_E(E)$ calculated according to Eq. (3) and the original data.

The difference between the measured and the calculated spectral count rate is less than 3% in the entire spectral region between 0.9–4 keV. The differences show some systematical features in their spectral dependence, which may be caused by uncertainties in the atomic absorption data used for the calculation of the quantum detection efficiency. In our calculation, e.g., the x-ray absorption fine structure which is very pronounced just above the Si K absorption edge has not been taken into account. In this spectral region the uncertainty of $\epsilon(h\nu)$ therefore is larger than 3%.

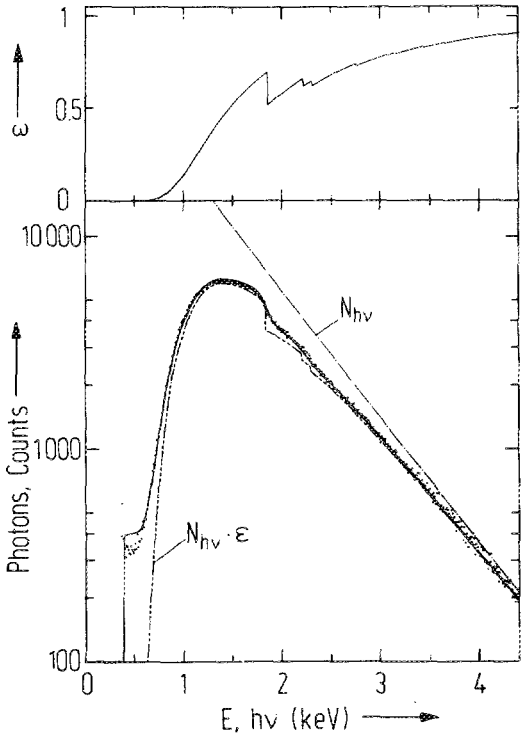

FIG. 5. Upper part: Quantum detection efficiency $\epsilon(E)$ calculated according to Eq. (5). Lower part: Calculation of the spectral counts rate $C_E(E)$ according to Eq. (3): $N_{h\nu}(h\nu)$ is the number of synchroton radiation photons entering the aperture in front of the detector, the full line is the convolution of $N_{h\nu}(h\nu)\epsilon(h\nu)$ according to Eq. (3). Dots are original data taken with the detector system. All curves refer to an integration time of 1000 s, a channel width of the MCA of 9.01 eV, BESSY operated with two electrons stored.

III. CONCLUSION AND OUTLOOK

We have shown that with the techniques presented in this paper a Si(Li) detector can be completely characterized in the spectral region between 0.9–5 keV. The absolute determination of photon fluxes with such a completely characterized system is possible with an uncertainty of less than 5%, which is much better than uncertainties achieved with other techniques in this spectral region.

We will use our completely characterized Si(Li) detector mostly for radiometric purposes, i.e., the measurements of the spectral responsivity of detectors like semiconductor photodiodes[17] and of the spectral emission of secondary standard radiation sources like Al K fluorescence excited by a radioactive Fe-55 source. It will also be utilized for the characterization of monochromators operated with synchrotron radiation.

ACKNOWLEDGMENT

We thank U. Kroth for experimental assistance.

[1]F. Riehle, E. Tegeler, and B. Wende, SPIE **733**, 486 (1986).
[2]D. D. Cohen, X-ray Spectrom. **16**, 237 (1987).
[3]J. L. Campbell and P. L. McGhee, Nucl. Instrum. Methods A **248**, 393 (1986).
[4]F. Riehle and B. Wende, Metrologia **22**, 75 (1986).
[5]J. Feldhaus, F. Schäfers, and W. Peatman, SPIE **733**, 242 (1987).
[6]J. L. Campbell, B. M. Millman, J. A. Maxwell, A. Perujo, and W. J. Teesdale, Nucl. Instrum. Methods B **9**, 71 (1985).
[7]Y. Inagaki, K. Shima, and H. Maezawa, Nucl. Instrum. Methods B **27**, 353 (1987).
[8]P. R. Bevington, *Data Reduction and Error Analysis for the Physical Sciences* (McGraw-Hill, New York, 1969).
[9]M. Geretschläger, Nucl. Instrum. Methods B **28**, 289 (1987).
[10]R. G. Musket, NBS Special Publication No. 604, edited by K. F. J. Heinrich, D. E. Newbury, and R. L. Myklebust, Gaithersburg, 1981, pp. 97–126.
[11]G. I. Johannsen, X-ray Spectrom. **11**, 194 (1982).
[12]J. L. Campbell, A. Perujo, and B. M. Millman, X-ray Spectrom. **16**, 195 (1987).
[13]W. Maenhaut and H. Raemdonck, Nucl. Instrum. Methods B **1**, 123 (1984).
[14]F. Riehle and B. Wende, Optik **75**, 142 (1987).
[15]W. S. Veigele, At. Data Nucl. Data Tables **5**, 51 (1973).
[16]B. L. Henke, P. Lee, T. J. Tanaka, R. L. Shimabukuro, and B. K. Fujikawa, At. Data Nucl. Data Tables **27**, 1 (1982).
[17]M. Krumrey, E. Tegeler, R. Thornagel, and G. Ulm (these proceedings).